Supplementary Information

Vapor-triggered Reversible Crystal Transformation in Nickel-based Magnetic Molecular Switch

Shufang Xue*, Gideon F.B Solre, Xiaoqin Wang, Liang Wang, Yunnan Guo*

Department of Chemistry, Key Laboratory of Surface & Interface Science of Polymer Materials of Zhejiang Province, Zhejiang Sci-Tech University, Hangzhou 310018, China. E-mail: yunnanguo@zstu.edu.cn; sfxue@zstu.edu.cn

Experimental section

General information. All chemicals used throughout the experiments were commercially available with analytical grade and used as received without any further purification, where all manipulations were also performed under an aerobic environment.

Synthesis of the ligand H_3sih. *N*-salicylisonicotinohydrazide H_3**sih** were prepared using literature procedures.[1]

Synthesis of complex 1: To a mixture of methanol and pyridine (7 mL, 4:3, v/v) solution of H_3**sih** (0.0620 g, 0.25 mmol) was added $Ni(OAc)_2.4H_2O$ (0.0806 g, 0.325 mmol) at room temperature. The resulting mixture was stirred for 10 min and it turned brown. After filtration, the solution was allowed to stand at room temperature for four days whereupon a brown prism crystal formed which was collected by filtration and washed with MeOH and dried in air. Yield 0.067 g, (83%, based on Ni). Anal. Calcd. (Found) for 1 ($C_{66}H_{56}N_{14}O_6Ni_3$): C, 60.15 (58.96); H, 4.28 (3.31); N, 14.88 (13.73).

Synthesis of complex 2: To a DMF solution (7 mL) of H_3**sih** (0.0643 g, 0.25 mmol)

was added $Ni(OAc)_2.4H_2O$ (0.0620 g, 0.25 mmol) in the presence of pyridine (0.5 ml) at room temperature. After stirring for 10 mins, the solution was filtrated and then exposed to air to allow the slow evaporation of the solvent. After standing for 20 days at room temperature, the red crystals were obtained from the filtrate. Yield 0.051 g, (80%, based on Ni). When single crystals of **1** (0.100 g, 0.155 mmol) were exposed in DMF vapor, which also yielded red crystals of **2** within two weeks at room temperature. Yield: 0.065 g (64%). Anal. Calcd. (Found) for **2** with empirical formula of $C_{42}H_{44}N_{10}O_{10}Ni_3$ (for 2 DMF and 2 H_2O per formula): C, 49.22 (48.96); H, 4.33 (3.31); N, 13.67 (12.73).

Characterization techniques. All chemicals were used as commercially obtained without further purification. Elemental analysis for carbon, hydrogen, and nitrogen were carried out on a Perkin-Elmer 2400 analyzer. Solution-state ^1H NMR spectra were recorded at room temperature on a Bruker Avance II 400 MHz spectrometer. The samples were dissolved in CD_3OD-d_4. Thermogravimetric analyses were conducted using a Rigaku Thermo plus EVO TG 8120 under Ar flow (0.3 L min^{-1}). Powder X-ray diffraction (PXRD) measurements were performed using Cu Kα radiation (λ = 1.5418 Å) on a DX-2700 X-ray diffractometer. Magnetic susceptibilities were measured on a Quantum design MPMS-5s SQUID magnetometer. The magnetic data were corrected for the sample holder and diamagnetic contributions. The crystal sample was quickly loaded into a gelatin capsule and immediately inserted within the SQUID cavity. Diffuse reflectance spectra (DRS) were obtained with a Shimadzu UV-2600 spectrophotometer equipped with a 60 mm integrating sphere and converted into absorption spectra by using the Kubelka–Munk function, using BaSO4 as a reference.

Crystal transformation between 1 and 2

Fresh single crystals of **1** or **2** were placed in a small glass vial, where an open-mouthed centrifugal tube containing corresponding solvent inserted. The whole assembly was sealed and allowed to stay until crystals turns to colors thanks to vapor diffusion. This setup can be launched to the Gouy balance for monitoring the

magnetic susceptibility change based on CISSS. Meanwhile, the color-changed sample was collected, then ground for the DRS and PXRD measurement. All the samples can be saturated under different vapor with sufficient time, without the observation of dissolving by the overload of vapor diffusion.

The measurement of *in situ* magnetic susceptibility (χ_M)

χ_M for monitoring the CISSS was measured by Faraday method, the magnetic force is defined by:

$$f_x = m\chi H_0 \frac{dH}{dx} \text{ and } \chi_M = \frac{M\chi}{\rho} \qquad (1)$$

in which, m = mass of sample; χ = volume magnetic susceptibility; H_0 = magnetic field strength at sample site; dH/dx = the field gradient along magnetic force direction.

On the other hand, the magnetic force can be obtained by the change of Gouy balance before and after magnetic field applied.

$$f_x = (\Delta W_{S+V} - \Delta W_V)g \qquad (2)$$

ΔW_{S+V} = apparent difference of **V**ial with **S**ample after and before magnetic field applied; ΔW_V = apparent difference of empty **V**ial after and before magnetic field applied; g = gravitational acceleration.

Combining equation (1) and (2) can deduct the final χ_M value for the corresponding samples. In our experiment, $FeSO_4 \cdot 7H_2O$ was used for a calibration, whose χ_M = 1.02E-2 cm_3/mol at RT; ρ = 1.895 g/cm^3. The density data of **1** and **2** are obtained from crystallographic calculations as shown in CIF.

Crystal data collection and structure refinement

Crystallographic data for complex **1** (at 293 K) and **2** (at 101 K) were collected using Mo-K_α (λ = 0.71073 Å) and Cu-K_α (λ = 1.54178 Å) radiation, respectively. The crystals were selected, mounted in inert oil and transferred to the cold gas stream for flash cooling. Data were integrated by CrysAlisPro 1.171.41.64a (Rigaku Oxford

Diffraction, 2020). Empirical absorption correction using spherical harmonics, implemented in SCALE3 ABSPACK scaling algorithm. Absorption correction was applied using the integrated multi-scan absorption algorithm. The structures were solved by direct methods (SHELXS) and refined by full-matrix least-squares on F^2 using SHELXL2014 and ShelXL 2018/3.[3] The location of the Fe atom was easily determined, and O, N, and C atoms were subsequently located in the difference Fourier maps. The non-hydrogen atoms were refined anisotropically. The H atoms were introduced in calculated positions and refined with fixed geometry with respect to their carrier atoms. Although solvent molecules per cell are actually be located, some of the lattice solvent molecules were disordered and could not be modeled properly; thus, program SQUEEZE,[4] a part of the PLATON package of crystallographic software, was used to calculate the solvent disorder area and remove its contribution to the overall intensity data. A solvent mask was calculated and 432 electrons were found in a volume of 1342 Å^3 in **2** void per unit cell. This is consistent with the presence of two DMF and two H_2O molecules per formula unit which account for 400 electrons per unit cell. CCDC 2117582 (**1**) and 2117583 (**2**) are the supplementary crystallographic data for this paper. They can be obtained free of charge from the Cambridge Crystallographic Data Center via www.ccdc.cam.ac.uk/data_request/cif.

Table S1. Crystal data collection and structure refinement parameters

Complex	**1**	**2**
Molecular formula	$[Ni_3(\mathbf{sih})_2(py)_8]$	$[Ni_3(\mathbf{sih})_2(py)_2]\cdot 2DMF\cdot 2H_2O$
Empirical formula	$C_{66}H_{56}N_{14}Ni_3O_6$	$C_{42}H_{44}N_{10}O_{10}Ni_3$
Formula weight	1317.37	1025.00
T/K	293(2)	101(2)
Crystal system	monoclinic	orthorhombic
Space group	*C*2/*c*	$C222_1$
a (Å)	17.8672(5)	13.0738(2)
b (Å)	16.8982(4)	22.4600(5)
c (Å)	20.9189(6)	14.5070(2)
α (º)	90	90
β (º)	101.260(3)	90
γ (º)	90	90
Volume/Å^3	6194.3(3)	4259.80(13)
Z	4	4
D_{calc} (g/cm^3)	1.413	1.598
μ/mm^{-1}	0.967	2.146
F(000)	2728.0	1720.0
Crystal size/mm^3	0.26 × 0.24 × 0.2	0.24 × 0.22 × 0.18
θ Range /°	3.97 to 58.85	3.97 to 75.895
Reflections collected	22145	11623
Independent reflections (R_{int})	6830(0.0197)	4335 (0.0689)
GOF on F^2	1.066	1.063
Final *R* indexes [$I>=2\sigma(I)$]	R_1= 0.0305, wR_2= 0.0759	R_1= 0.0691, wR_2= 0.1778
Final *R* indexes [all data]	R_1= 0.0417, wR_2= 0.0801	R_1= 0.0789, wR_2= 0.1879
Largest diff. peak/hole /e Å^{-3}	0.25/-0.22	1.05/-0.82

Table S2. Bond lengths (Å) and angle (º) for complexes **1** and **2**

Complex 1				Complex 2			
Ni1-O2	1.997(12)	Ni2-O1	2.036(12)	Ni1-O2	2.009(4)	Ni2-O1	1.824(4)
Ni1-N2	2.129(12)	Ni2-O3	1.983(13)	Ni1-N2	2.130(5)	Ni2-O3	1.830(5)
Ni1-N4	2.184(2)	Ni2-N3	1.979(13)	Ni1-N4	2.107(6)	Ni2-N3$^{\#}$	1.927(5)
Ni1-N5	2.159(2)	Ni2-N6	2.195(14)	Ni1-O2*	2.009(4)	Ni2-N1	1.830(5)
Ni1-O2*	1.997(12)	Ni2-N7	2.175(15)	Ni1-N2*	2.130(5)		
Ni1-N2*	2.129(12)	Ni2-N8	2.102(15)	Ni1-N4*	2.107(6)		
O2-Ni1-O2*	177.84(7)	O1-Ni2-O3	171.87(5)	O2-Ni1-O2*	178.6(3)	O1-Ni2-N1-	94.1(2)
O2-Ni1-N2	78.67(5)	O1-Ni2-N3	79.2195)	O2-Ni1-N4	91.4(2)	O1-Ni2-O3	178.6(2)
O2*-Ni1-N2	101.25(5)	O1-Ni2-N6	88.04(5)	O2-Ni1-N4*	87.7(2)	O1-Ni2-N1	94.1(2)
O2-Ni1-N2*	101.26(5)	O1-Ni2-N7	88.57(5)	O2*-Ni1-N4	87.7(2)	N1-Ni2-O3	84.6(2)
O2*-Ni1-N2*	78.67(5)	O1-Ni2-N8	95.14(5)	O2*-Ni1-N4*	91.4(2)	O1-Ni2-N3$^{\#}$	88.8(2)
O2*-Ni1-N4	91.08(4)	O3-Ni2-N3	92.67(5)	N4-Ni1-N4*	91.2(3)	N1-Ni2-N3$^{\#}$	176.9(2)
O2-Ni1-N4	91.08(4)	O3-Ni2-N6	92.14(5)	O2-Ni1-N2*	102.8(2)	O3-Ni2-N3$^{\#}$	92.5(2)
O2*-Ni1-N5	88.92(4)	O3-Ni2-N7	92.16(6)	O2*-Ni1-N2	102.8(2)		

O2-Ni1-N5	88.92(4)	O3-Ni2-N8	92.98(6)	O2-Ni1-N2	78.09(19)
N2*-Ni1-N2	175.96(7)	N3-Ni2-N6	89.93(5)	O2*-Ni1-N2*	78.09(19)
N2*-Ni1-N4	92.02(3)	N3-Ni2-N7	96.02(6)	N4-Ni1-N2*	165.63(19)
N2-Ni1-N4	92.02(3)	N3-Ni2-N8	172.60(6)	N4*-Ni1-N2*	87.3(2)
N2-Ni1-N5	87.98(3)	N6-Ni2-N7	172.49(6)	N4-Ni1-N2	87.3(2)
N2*-Ni1-N5	87.98(3)	N6-Ni2-N8	85.09(6)	N4*-Ni1-N2	165.63(19)
N5-Ni1-N4	180.0	N7-Ni2-N8	88.54(6)	N2-Ni1-N2*	97.6(3)

Symmtery code:*:1-*x*, *y*, 0.5-*z*;#: 0.5-*x*, 0.5-*y*, -0.5+*z*.

Table S3. Analysis of C-H...Cg Interactions of complex **1**

D-H…*Cg*[a]	Symmetry code	H…*Cg*	D-H..*Cg*	D…*Cg*
C22-H22…*Cg*11	1/2-*x*,1/2+*y*,1/2-*z*	2.61	161	3.506(2)
C27-H27…*Cg*11	1/2-*X*,-1/2+*Y*,1/2-*Z*	2.79	159	3.666(2)

[a]*Cg*11 is the centroid of the C8-C13 ring.

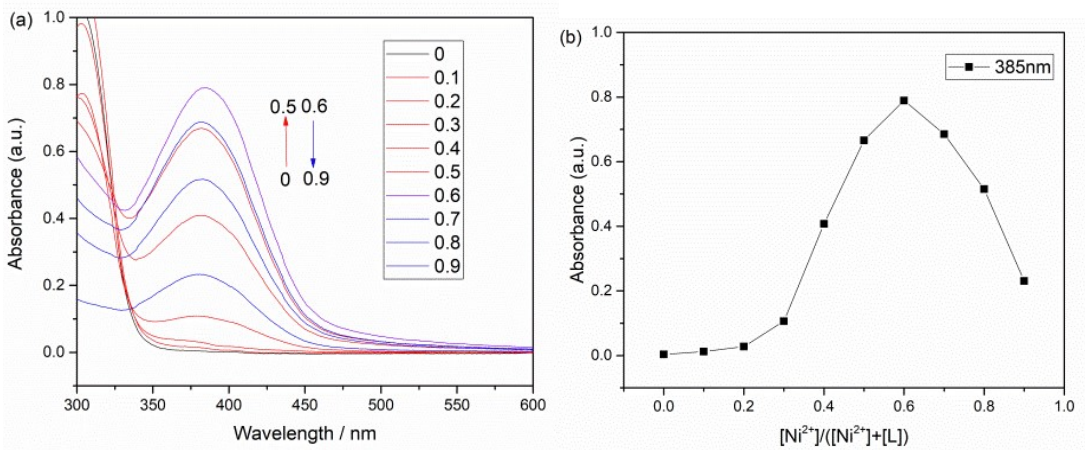

Fig. S1 (a) The absorption spectra changes of HL in DMF solution (C = 2.0× 10^{-4} mol L^{-1}) with Ni^{2+}. (b) The absorption spectra changes of $[Ni^{2+}]/([Ni^{2+}]+[L])$and the emission intensity curve at 385 nm. When the mole fraction of $[Ni^{2+}]/([Ni^{2+}]+[H_3L])$ was around 0.6, the absorbance of solution achieved the maximum, insinuating that the complex ratio of Ni^{2+} and H_3L was 3:2 (C = 2.0 × 10^{-4} mol/L)

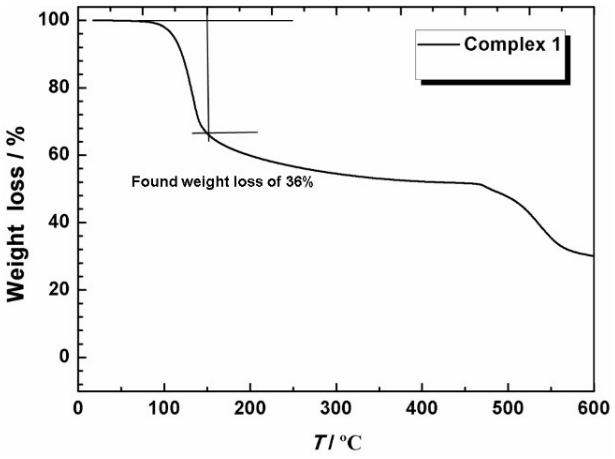

Fig. S2 TGA curves for complex **1** under an Ar(g) flow at 10℃/min.

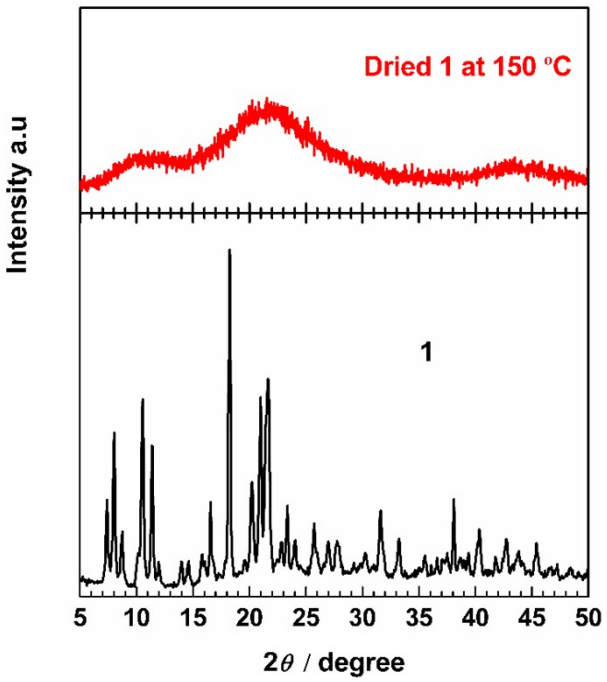

Fig. S3 PXRD patterns for complex 1(black) and dried sample **1** (red) at 150℃.

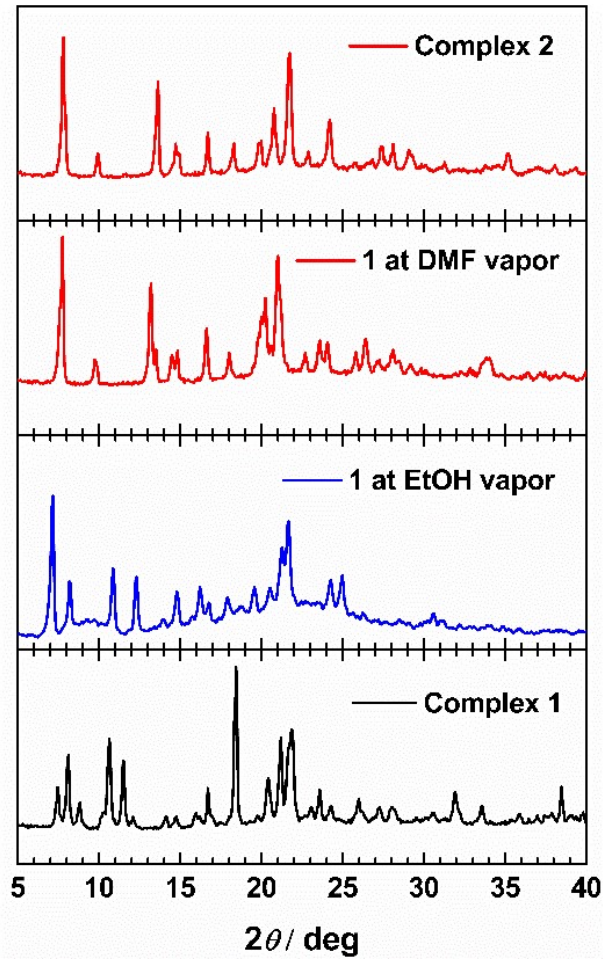

Fig.S4 Comparison of PXRD patterns at different vapor within two weeks.

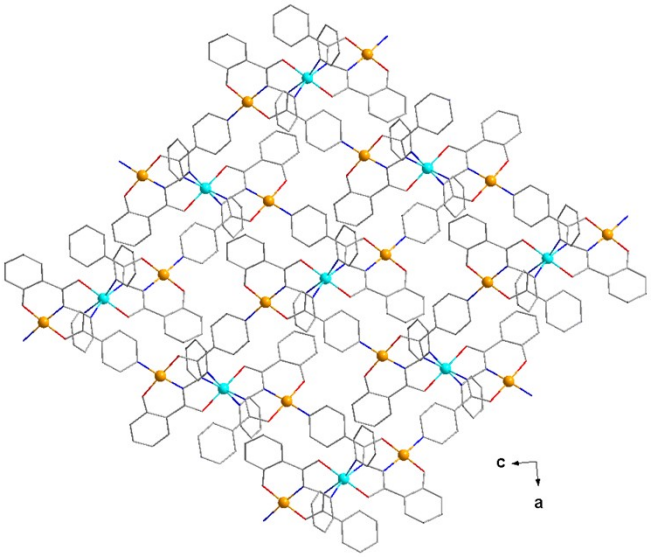

Fig.S5 2D polymeric network of **2**. Color code: grey (C), blue (N), pink (O), cyan (HS Ni^{II}) and orange (LS Ni^{II}).

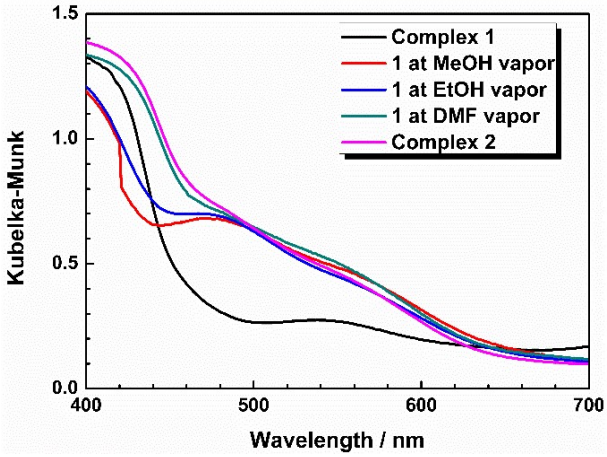

Fig. S6 Vapochromic behavior in the diffuse reflectance spectrum exposure to corresponding vapors.

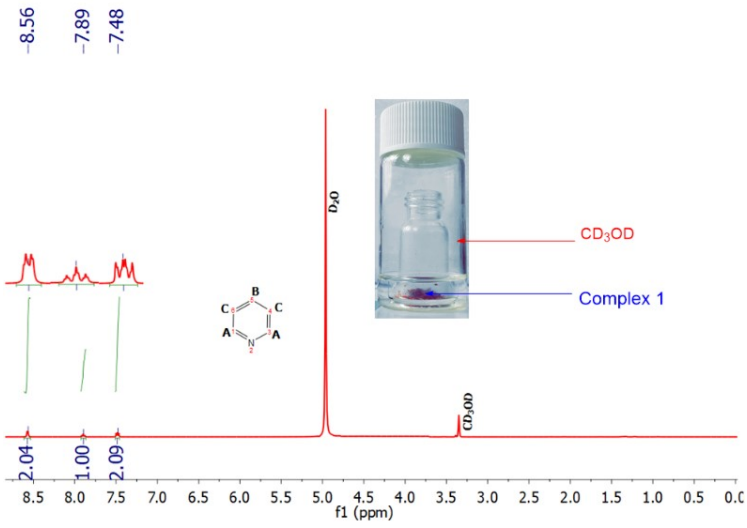

Fig. S7 ^{1}H NMR spectra confirming the decomposition of pyridine molecule during the vapochromic cycle.

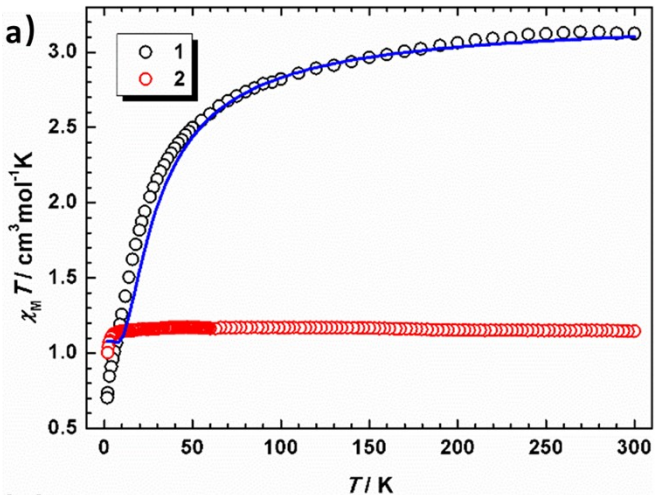

Fig. S8 Thermal variation of the $\chi_M T$ product per Ni_3 for complex **1** and **2**. Solid blue line represents the best fit to the model.

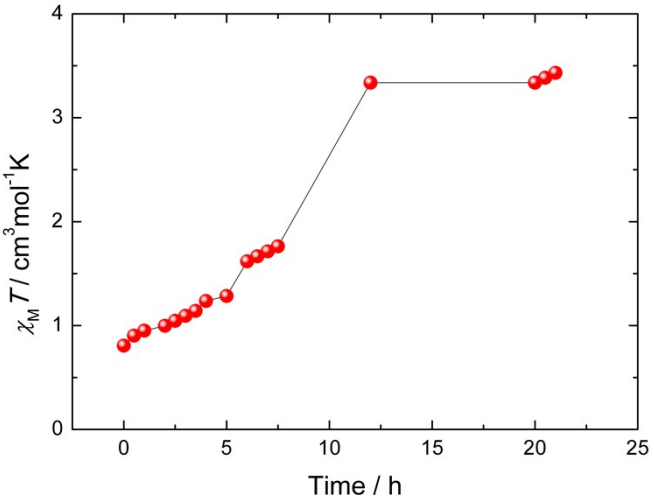

Fig. S9 Time-dependent magnetic switch of complex **2** under pyridine vapor.

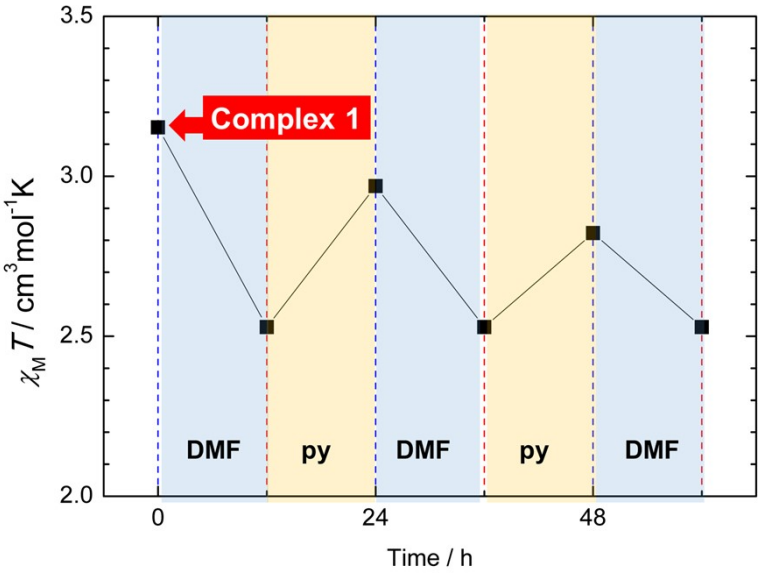

Fig. S10 Reversible magnetic switch during different vapor diffusion at *in situ* Gouy Balance starting from complex **1**.

Reference:

1. Y.-X. Zhou, R.-F. Yuan, C.-L. Fan, L.-E. Liu, B.-L. Wu and H.-Y. Zhang, *J. Coord. Chem.*, 2012, 65, 3133.
2. O. Kahn, Molecular Magnetism, Wiley-VCH, New York, 1993.
3. G. Sheldrick, *Acta Crystallogr., Sect. A*, 2008, 64, 112-122.
4. A. L. Spek, *Acta Crystallogr., Sect. A: Fundam. Crystallogr.*, 1990, 46, C34.